THERMOPHYSICAL PROPERTIES AND HEAT TRANSFER CHARACTERISTICS OF $CaCl_2$ HEAT PUMP REACTOR ASSOCIATED WITH STRUCTURAL CHANGE OF REACTIVE SALTS

Yushi Hirata
Division of Chemical Engineering
Graduate School of Engineering Science
Osaka University
Toyonaka 560-8531, Japan
+81-6-6850-6275 / +81-6-6850-6277 ; hirata@cheng.es.osaka-u.ac.jp

Keiko Fujioka
Shinsei Cooling Water System Co., Ltd.
501 Toa bldg., 1-3-22 Kyomatibori, Nishi-ku, Osaka 550-0003, Japan
+81-6-6445-5433 / +81-6-6445-5452 ; kfujioka@shinsei-uwtb.co.jp

Abstract

This paper presents the results obtained in our investigations on thermophysical properties of a $CaCl_2$ salt formed by the reaction with ammonia, methylamine or methanol gas and heat transfer characteristics in a bed packed with $CaCl_2$ salt. Volume and heat capacity of a $CaCl_2$ salt thus prepared were measured by the gas-displacement method and the differential scanning calorimetry (DSC), respectively. A comprehensive investigations on literature data as well as our data reveals that the increases in volume and heat capacity of a salt are inherent in each substance absorbed in the salt by reaction and they are expressed by the additivity of the properties of the unreacted salt to those of the absorbed substance in a condensed phase. Measurements of effective thermal conductivity were performed for a packed bed of $CaCl_2$ salt formed in a slender glass vessel equipped with thermocouples. The effective thermal conductivity was reduced by reaction to less than a half that of the initial anhydrous $CaCl_2$ bed. A model to estimate effective thermal conductivity of a bed packed with porous pellets and pellet thermal conductivity is proposed by extending the previous models proposed by Kunii and Smith, Okazaki et. al., and Luikov et al. The equations derived from the model represent appropriately the effects of gas pressure, gas thermal conductivity and void fraction on the effective thermal conductivity. In addition, the model expresses well a significant decrease in the pellet thermal conductivity due to reaction by taking account of the changes in structure of agglomerated grains in a pellet in terms of contact resistance to heat transfer through it.

KEYWORDS

Chemical heat pump, Packed bed reactor, Calcium chloride, Ammonia, Methanol, Methylamine, Molar Volume, Molar heat capacity, Effective thermal conductivity,

1. INTRODUCTION

In research and development of chemical heat pumps to upgrade low level thermal energy by utilizing reversible gas-solid reactions, characteristics of heat transfer in the reactor must be taken into account, since heat transfer plays an important role in promoting the overall reaction rate.

Reversible gas-solid reactions utilized for driving heat pumps are generally expressed by

$$A{\cdot}mB\ (\text{solid}) + nB(\text{gas}) = A{\cdot}(m+n)B(\text{solid}) \quad (1)$$

Absorption or desorption reaction with the gas substance accompanies expansion or contraction of the reactive salt. This also causes variations in thermophysical properties of the salt, such as density, heat capacity and thermal conductivity. Since the overall reaction rate in a packed bed reactor, which is ordinarily used as a reactor for gas-solid chemical heat pump, is likely to be controlled by heat transfer, knowledge on thermophysical properties of a salt formed or decomposed by reaction and heat transfer characteristics in a bed packed with the salt is indispensable for designing a reactor bed or analyzing its performance.

The following studies have been reported concerning the variations of volume and heat capacity of reactive salts. Gillespie and Gerry [1] reported the densities of reactive solids of $CaCl_2/NH_3$ and $BaCl_2/NH_3$ systems, and Mauran et al [2] reported the molar volume of $CaCl_2{\cdot}n CH_3NH_2$ (n=2 and 6) and $MnCl_2{\cdot}nNH_3$ (n=2 and 6).

Oms [3] and Goetz and Marty [4] pointed out that large variations in volume of the reactive salts affect the heat transfer properties of the bed in $CaCl_2/CH_3NH_2$ and $MnCl_2/NH_3$systems. Lourdudoss et al. [5] and Marty [6] carried out DSC measurements on heat capacities of $CaCl_2{\cdot}nNH_3$(n=1, 2, 4 and 8) and $MnCl_2{\cdot}nNH_3$ (n=2 and 6), respectively. Several attempts have been made to measure the heat capacity without using DSC. For example, Oms [3] determined the heat capacity of $CaC1_2 \cdot nCH_3NH_2$ (n=2 and 6) by applying the parameter fitting method to the unsteady temperature changes measured in a reactor bed. Mazet and Amouroux [7] and Goetz and Marty [4] mentioned that the heat capacity of reactive salt in $MnC1_2/NH_3$ and $CaC1_2/CH_3NH_2$ systems might be estimated by the sum of heat capacity of the salt and that of the reactant in gas state.

As for heat transfer in reactor beds, its enhancement has attracted more attention than the study of effective thermal conductivity, since it is more directly applicable to improving the reactor performance. For example, Oms [3] and Mauran et al. [2] investigated the effective thermal conductivities of the $CaCl_2/CH_3NH_2$ and $MnCl_2/NH_3$ reactor beds in which graphite was mixed to promote heat transfer. Guilleminot [8] reported improvements of thermal conductivity by use of consolidated adsorbents of metallic foam and zeolite. Groll [9], Kanzawa and Arai [10] and Ogura et al. [11] studied the effects of inserting metal plates, foams, wires or fins on heat transfer and reactor performance.

In the ordinary operation of gas-solid reaction, porous pellets of solid reactant are used to enhance the overall reaction rate, and the structure and dimensions as well as thermophysical properties of the porous pellet reactant will change as the reaction proceeds. In addition, the temperature and pressure in the reactor has to be changed in order to reverse the reaction. These factors must influence not only the heat transfer but also the reaction progress in a packed bed reactor that is normally used for a gas-solid chemical heat pump. Without adequate knowledge about these items, it will be impossible to develop a high performance reactor based on quantitative analysis.

We have been conducting a systematic study on thermophysical properties and heat transfer characteristics for $CaCl_2$ packed beds, since $CaCl_2$ is applicable to driving a heat pump by combining its reaction with ammonia, methylamine or methanol gas with the phase change of one of theses fluids. This paper describes how the volume and heat capacity of a $CaCl_2$ salt as well as the effective thermal conductivity of a bed packed with the porous reactive pellets change during reaction and how the variations of thermophysical properties and effective thermal conductivity are quantitatively correlated and expressed.

2. VOLUME OF REACTIVE SALT

2.1 Expansion/Contraction of Bed Volume

Volume changes of a bed of $CaC1_2{\cdot}nNH_3$ salt formed in a glass vessel are shown in Fig. 1. In the initial absorption reaction (a → b), the bed volume increased by about four times that of anhydrous $CaC1_2$ bed by absorbing 7.9 moles of ammonia in one mole of calcium chloride. During the following adsorption/desorption reaction cycles (b ↔ c), the volume change becomes fairly small

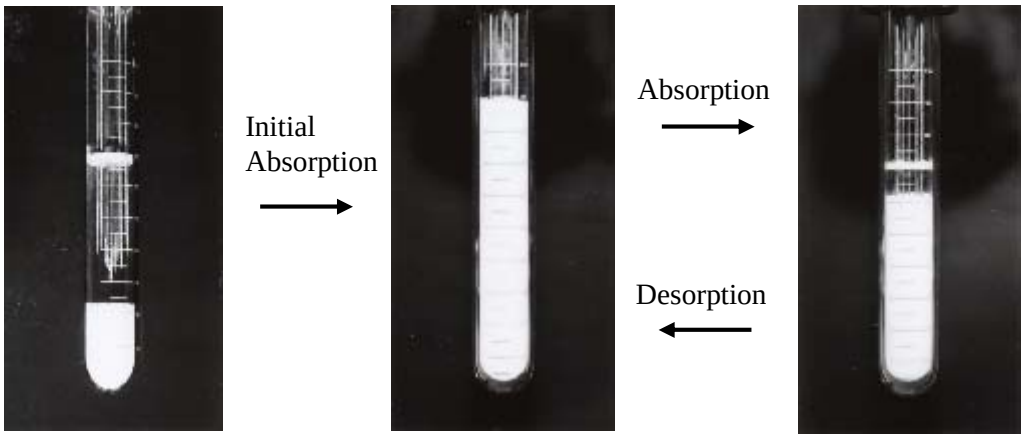

(a) n=0 (b) n=7.9 (c) n=2.1

Fig.1 Volume expansion and contraction of the bed of $CaCl_2{\cdot}nNH_3$

compared with the initial expansion.

Figure 2 shows the variation of bed volume V_b with n for a $CaC1_2 \cdot nCH_3OH$ bed during the first three reaction cycles. At the end of the initial absorption reaction, the bed volume has expanded to about double the initial volume of anhydrous $CaC1_2$ bed, V_{b0}. But contraction in the subsequent desorption reaction does not follow the same path in the initial adsorption and the volume expansion ratio V_b/V_{b0} is 1.7 when the reaction is completed at n = 0. During the subsequent two reaction cycles V_b increased slightly as whole. After the third cycle the variation of V_b with n follows almost the same path between V_b/V_{b0} = 2 and V_b/V_{b0} = 2.5 during adsorption/desorption reaction. Similar variations of the bed volume were observed for $CaCl_2/CH_3NH_2$ reaction system, in which the initial expansion was V_b/V_{b0} = 4.

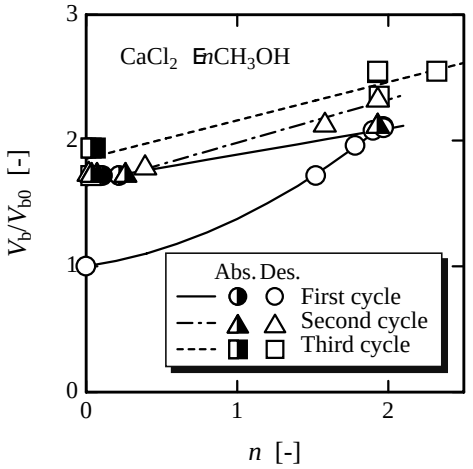

Fig.2 Variation of bed volume of CaC… with n.

Such a large irreversible expansion of the bed volume, which may occur during the initial adsorption reaction as described above, must be taken into account in preparing a reactor bed by packing pellets of anhydrous $CaCl_2$ or a solid reactant.

2.2 Molar Volume of Reactive Salt

Volume of particles is usually determined from the displaced volume of liquid using a pycnometer, but this method may not be applicable to a highly reactive salt because it is difficult to find inert liquids suitable for it. Moreover, a reversible reactive salt is easily decomposed to release the absorbed gas when the gas pressure becomes lower than the equilibrium pressure for the reaction. To avoid such decomposition, we adopted the gas-displacement method to measure the volume of reactive salts [12].

Anhydrous $CaCl_2$ particles of known weight, which was put in a gas-tight vessel, were exposed to a reactive gas to prepare a sample salt. The total weight of the vessel was measured to determine the amount of the gas substance reacted with $CaCl_2$. Then inert gas of N_2 or Ar was supplied into the vessel, and the total weight of the vessel and the gas phase pressure were measured. The amount of the inert gas supplied was obtained from the increase in the total weight. This procedure was repeated to obtain a relation between the amount of the inert gas and the gas phase pressure, to which the ideal gas law was applied to derive the volume of the gas phase in the vessel. Finally, the volume of the reactive salt was obtained by subtracting the volume of gas phase from the empty vessel volume. In this way, the volume measurements were carried out for the $CaCl_2$ salt that had completed the absorption or desorption reaction; n=2 or 6 for $CaCl_2 \cdot nCH_3NH_2$, n=8 or 2 for $CaCl_2 \cdot nNH_3$ and n=2 for $CaCl_2 \cdot nCH_3OH$, at room temperature.

Figure 3 shows how the molar volume of $CaCl_2$ salt increases with the amount of gas substance absorbed in it by reaction. The increase in the

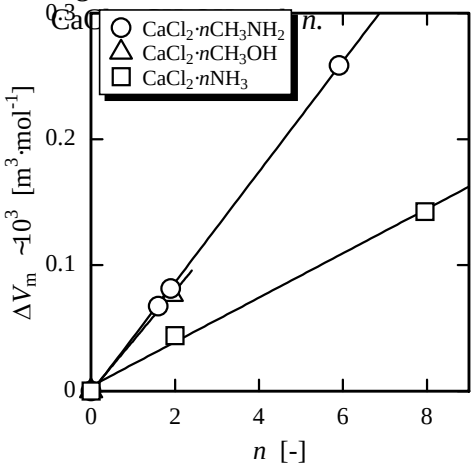

Fig.3 Increase in molar volume of reactive salts with n.

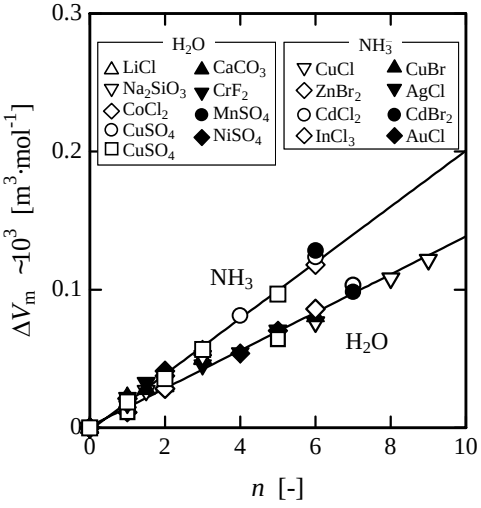

Fig.4 Increase in molar volume of hydrates and ammoniates with n.

molar volume is expressed by $\Delta V_m = V_m(n) - V_m(0)$, where n denotes the mole of gas substance reacted with one mole of $CaCl_2$ and $V_m(0) = 50.5$ cm^3 mol^{-1} is the molar volume of anhydrous $CaC1_2$. For each reaction system $\Delta V_m(n)$ increases in proportion to n and expressed by

$$\Delta V_m = V_m(n) - V_m(0) = \beta n \qquad (2)$$

where $\beta = 43.6 \times 10^{-6}$ m^3 mo^{-1} for $CaCl_2 \cdot n CH_3NH_2$, $\beta = 39.8 \times 10^{-6}$ m^3 mol^{-1} for $CaCl_2 \cdot n CH_3OH$ and $\beta = 19.0 \times 10^{-6}$ m^3 mol^{-1} for $CaCl_2 \cdot n NH_3$.

By analyzing literature data [13], it has been confirmed that the validity of the linear relationship of eq. (2) holds for other reaction systems. Figure 4 shows variations of ΔV_m with n for various inorganic hydrates and ammoniates. The volume of hydrates or ammoniates varies linearly with the amount of water or ammonia reacted with the salts, and the increase in volume of the reactive salt does not depend on the salt substance but on the amount of the substance absorbed in each salt. The values of βobtained from the slopes of the lines in Figs.4 are 14 x 10^{-6} m^3/mol for hydrates and 19 x 10^{-6} m^3/mol for ammoniates, respectively.

The coefficient β in eq. (2) represents the volume occupied by one mole of the gas substance absorbed in the salt. Hence it is reasonably presumed that the value of $\beta$is close to the molar volume of the absorbed substance in a condensed phase. Since the density data in solid state are not complete for the substances examined above, $\beta$is compared with the molar volume of each substance in liquid state; β is 87 % of the liquid molar volume of absorbed substance for $CaC1_2 \cdot n CH_3NH_2$, 99% for $CaC1_2 \cdot n CH_3OH$, 71% for $CaC1_2 \cdot n NH_3$, and 78 % for $CaC1_2 \cdot n H_2O$. The values are close to the liquid molar volume for methylamine and methanol but less than that for hydrates and ammoniates. This is probably due to the smallness in molecular sizes of water and ammonia in comparison with methylamine and methanol. In other words, water and ammonia may be more influenced by the surrounding atoms constituting the inorganic salt than methylamine and methanol are.

2.3 Structural Change of $CaCl_2$ Salt

Fujioka investigated structural deformation of $CaCl_2 \cdot n CH_3OH$ salt by taking SEM photographs of the salt completely reacted (n=2) or decomposed (n=0) [14]. The anhydrous $CaCl_2$ particles, which were used for preparing the salts, were agglomerates of fine round grains of $CaCl_2$ or porous pellets. After the initial adsorption/desorption reaction, SEM photographs showed that some of the adjacent grains partly fused to form a network-like structure but the rest grains almost reverted to the original shape. As the reaction was repeated, the grains in a pellet transformed from round to angularly slender. Such a large change in the structure of a grain can be seen in Fig.5, which compares the round shape of the initial anhydrous CaCl2 grains with angularly slender shape of the grain exposed to four reaction cycles. The length of the slender grains was several μm to about ten μm. Such deformation did not progress uniformly in a pellet and the degree of deformation varied locally even in the same pellet. But the pellet, as a whole, was closely packed with more grains with slender shape as the reaction was repeated.

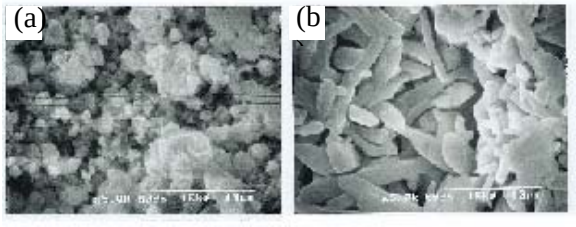

Fig.5 SEM Photographs of (a) $CaCl_2$ anhydride before reaction and (b) $CaCl_2$ salt after having completed the fourth desorption in the reaction with CH_3OH.

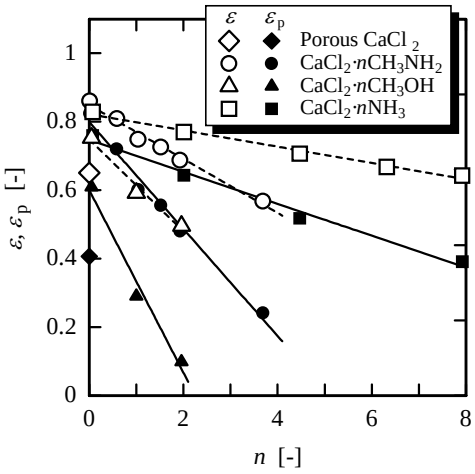

Fig.6 Variations of void fractions ε and ε_p with n.

2.4 Void Fractions of Bed and Pellet

The SEM observation mentioned above revealed that each $CaCl_2$ salt was a porous pellet composed of almost unporous grains. Therefore, a reactor

bed formed by packing such porous pellets should be characterized by two void fractions, i.e., bed void fraction ε_b, and pellet void fraction ε_p. The former represents the ratio of vacant volume surrounded by the pellets in the bed to the total bed volume and the latter represents the ratio of vacant volume in a pellet to its total volume. The overall void fraction, ε, is expressed by $\varepsilon = 1 - V_s/V_b$, where V_b is the bed volume and V_s is the real volume of solid phase. The bed void fraction is given by $\varepsilon_b = 1 - V_p/V_b$ with pellet volume V_p, and the pellet void fraction is given by $\varepsilon_p = 1 - V_s/V_p$. From these relations, the following expression holds among the three void fractions.

$$\varepsilon_p = (\varepsilon - \varepsilon_b)/(1 - \varepsilon_b) \quad (3)$$

Figure 6 shows how ε and ε_p in $CaCl_2$ salt beds formed in a glass vessel vary with reaction. The glass vessel was shaken sometimes to promote the reaction uniformly and then the bed height was measured after tapping the vessel several times on a stone table. Such a procedure may allow the bed to expand or contract freely during reaction. Hence it may be assumed that the bed void fraction ε_b does not change during reaction.

The keys for porous $CaCl_2$ denote the bed before reaction and the other keys denote the bed after several reaction cycles were repeated. At the anhydrous state n=0 the void fraction ε of the bed exposed to several reaction cycles is larger than that of the unreacted $CaCl_2$ bed, and it decreases with the progress of reaction or with increasing n. Such a decrease in ε is due to volume expansion of the salt by reaction. From the measurements of true density and pore size distribution of pellets with mercury porosimetry, ε_b=0.476 and ε_p=0.332 were obtained for the unreacted $CaCl_2$ bed. Using the assumption of constant ε_b, pellet void fraction ε_p was derived from the measured ε. The pellet void fraction decreases considerably with increasing n, as shown by the closed key in Fig.6.

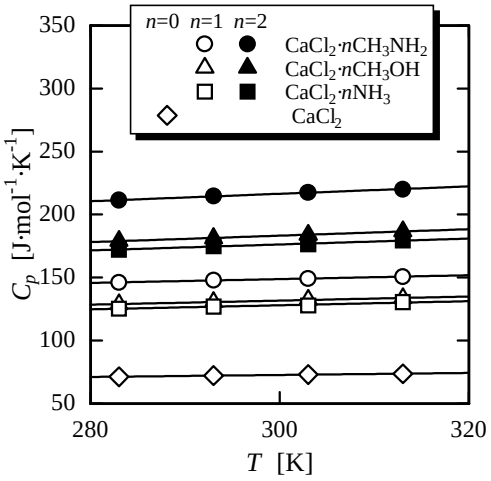

Fig. 7 Temperature dependence of heat capacity

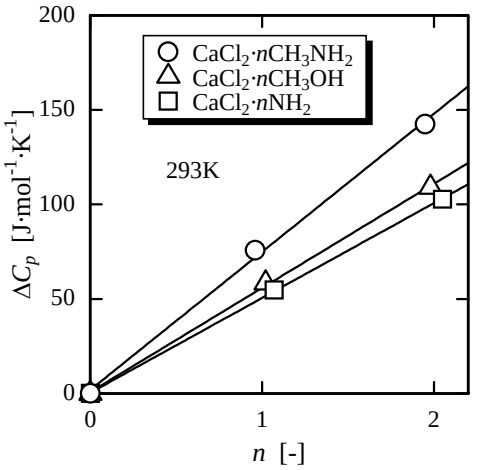

Fig.8 Increase in heat capacity of reactive salt with moles n of substance reacted with $CaCl_2$.

3 HEAT CAPACITY OF REACTIVE SALT

3.1 Increase in Heat Capacity of $CaCl_2$ Salt due to Reaction

Fujioka et al. measured heat capacity of $CaC1_2 \cdot nCH_3NH_2$, $CaC1_2 \cdot nNH_3$ or $CaC1_2 \cdot nCH_3OH$ by using DSC [12]. Since the salts with n larger than 2 are unstable and decomposed easily in the DSC operation to elevate the temperature, the measurements were carried out for the salts with n=1 or 2 by confirming that the DSC chart did not show any endothermic peaks indicating the possible desorption reactions.

Figure 7 shows that heat capacities of anhydrous calcium chloride and reactive salts increase slightly with temperature. The increase in heat capacity is 5 to 7% in the range from 283 K to 323 K, and the temperature dependence of the heat capacity is expressed by a straight line.

Figure 8 shows the linear relationship between the increase in molar heat capacity of the reactive salt, $\Delta Cp = Cp(n) - Cp(0)$, and n at 293 K. The increase in heat the capacity can be expressed by the following relation,

$$\Delta Cp = Cp(T,n) - Cp(T,0) = \gamma(T) \cdot n \quad (4)$$

where γ denotes an increase in heat capacity owing to the absorption of one mole of the reactive gas substance.

3.2 Additivity Law for Heat Capacity of Reactive Salt

The above-mentioned additivity for heat capacity can be generalized by using literature data [15]. Figure 9 shows the relation between ΔCp obtained from the literature data for hydrates at 250 K and moles of water reacted with one mole of the salt, n. Similarly to the results for $CaC1_2$ salts, ΔCp increases in proportion to n, and the data can be fitted by a straight line irrespective of the kinds of salts. In addition, it has been confirmed that the literature data satisfy the linear relation in the wide range from T=20K to 250K.

Lourdudoss et al. [5] and Marty [5] described that the heat capacity of the ammoniated salt could be expressed as the sum of the heat capacity of inorganic salt and that of ammonia in gas phase. It will, however, be more reasonable to consider that the heat capacity of the substance absorbed in a reactive solid is much the same as that in a condensed phase, since it may not behave freely in the confined space in the salt.

This issue has been investigated for hydrates. The values of γ for the hydrates obtained from the literature data are plotted together with the specific heat capacities of ice in Fig.10. In the temperature range of 20 K to 250 K, γ is almost equal to the heat capacity of water in solid phase or ice.

In Fig. 11, the values of γ for $CaCl_2$ salts for methylamine, methanol and ammonia systems are compared with the heat capacity of each substance in solid, liquid or gas phase. The heat capacities in liquid phase at a given temperature were obtained by interpolating the literature data and those in gas phase were calculated using the Rihani-Draiswamy equation. The heat capacities of solid methylamine, ammonia and methanol were estimated by applying Neumann-Kop's law. The law assumes that the heat capacity of a solid is equal to the sum of atomic heat capacities of its component element and is considered to be valid in the range above the Debye temperature where the heat capacity of solid hardly changes. Figure 11 shows that the value of γ for each $CaC1_2$ reactive salt is close to the heat capacity of the absorbed substance in solid phase. This is probably due to the situation in which the motion of the molecules of absorbed substance is strongly bounded by chemical bonding in the salt.

4. THERMAL CONDUCTIVITY

4.1 Measurements of Effective Thermal Conductivity

Measurements of effective thermal conductivity were carried out by using the glass vessel shown in Fig.1. Inside of the vessel thermocouples were placed in such an arrangement that the squares of the squares of the radial distance from the center to each position were equally spaced. Particles used for making packed beds were glass beads, pellets of nonporous and porous $CaCl_2$ and pellets of $CaCl_2{\cdot}n CH_3NH_2$, $CaCl_2{\cdot}n NH_3$ and

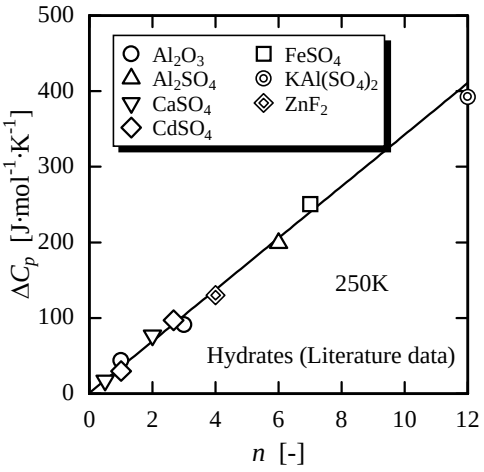

Fig.9 Increase in heat capacity of hydrates with moles n of H_20 reacted with salts.

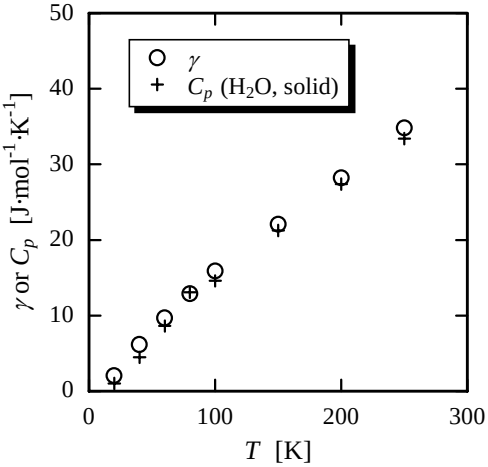

Fig.10 Temperature dependence of heat capacity increase of hydrates and heat capacity of H_2O(sold).

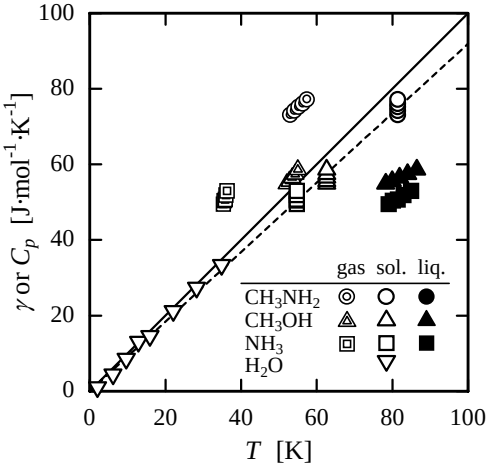

Fig.11 Comparison of heat capacity of $CaCl_2$ reactive salts with those of absorbed substance in solid, liquid and gas states

$CaCl_2 \cdot nCH_3OH$. Nonporous $CaCl_2$ pellets were prepared by crushing a solid lump of $CaCl_2$, which had been made by cooling a molten salt of commercial $CaCl_2$ powder. To prepare a bed composed of reactive pellets, the reaction of $CaCl_2$ with CH_3NH_2, CH_3OH or NH_3 was advanced until n reached a specified value after the pellets had been exposed to several absorption/desorption reaction cycles. Then the vessel containing the pellets of $CaCl_2$ salt was tapped several times to fix the bed in it. Hence the bed thus prepared can be regarded as a freely expanding or contracting one as described in 2.4. The mean diameters D_p of the sample particles are as follows, D_p=60, 100, 400 and 925 μm for glass beads, D_p=175, 400 and 675 μm for nonporous $CaCl_2$ pellets and D_p for the reactive pellets was estimated to vary between 300 μm and 400 μm.

The effective thermal conductivity of the bed was measured by the unsteady method. The vessel of the bed, which was kept at 273K in an ice water bath, was placed suddenly into another water bath at 293K. The effective thermal conductivity was obtained from the time variations of temperature distribution in the bed. The procedure to derive the effective thermal conductivity is described in detail in the paper by Fujioka et al. [16].

In the measurement accompanied with the step variation of temperature from 273 K to 293 K, the gas phase pressure was controlled so that neither adsorption nor desorption reaction took place in the bed. Equilibrium states of the salt are attained at n=2, 4 and 6 for the methylamine system, n=2 for the methanol system and n=2, 4, 8 for the ammonia system. The equilibrium pressure for the reactions between n=0 and 2 is so low that n of each reactive salt with $n \leq 2$ can be kept unchanged in the atmosphere of an inert gas. In the case of n>2, the reaction does not take place in the above mentioned temperature range provided that the pressure of reactive gas is kept almost nearly equal to the equilibrium pressure, P_e. In this manner the experiments for n>2 was conducted under the condition where the reactive salt was kept in one of the equilibrium states during measurement.

Effects of the amount of gas substance reacted with $CaCl_2$ on λ_{eff} were investigated at P=101.3 kPa. For $CaCl_2$ anhydride and reactive salts with $n \leq 2$, measurements were carried out in an atmosphere of N_2. As for the reactive salts with n>2, a certain amount of the reactive gas, which corresponds to the equilibrium pressure for each salt, exists in the vessel. To make a meaningful comparison, a mixture of N_2, He and Ar gases at 101.3 kPa was introduced into the vessel, whose thermal conductivity was adjusted to be equal to the thermal conductivity of N_2 at 101.3 kPa. In addition, in order to investigate pressure dependence of effective thermal conductivity, measurements were conducted for the bed packed with reactive pellets with $n \leq 2$, nonporous $CaCl_2$ pellets, porous $CaCl_2$ pellets and glass beads in the gas phase of inert gas of Ar, He or N_2 in the wide range of 5 Pa to 200 kPa.

4.2 Variations of Effective Thermal Conductivity

Figure 12 shows variations of λ_{eff} of $CaCl_2 \cdot nCH_3NH_2$, $CaCl_2 \cdot nCH_3OH$ and $CaCl_2 \cdot nNH_3$ beds with n in the gas phase with the same thermal conductivity of N_2 at 101.3 kPa, in which λ_{eff} of unreacted porous $CaCl_2$ bed is plotted for comparison. λ_{eff} of the reactive pellets with n=0, which had been prepared after exposing to several reaction cycles, was reduced to 1/3 ~ 1/2 of that of the unreacted $CaCl_2$. Generally λ_{eff} depends on pellet thermal conductivity λ_p, gas thermal conductivity and void fraction. Since the data in Fig.12 were obtained under the same pressure and thermal conductivity of gas phase, the difference in λ_{eff} will be attributed to the remaining two factors, λ_p and the pellet void fraction ε_p, since the bed void fraction ε_b could be assumed unchanged due to the free expansion or contraction of the bed.

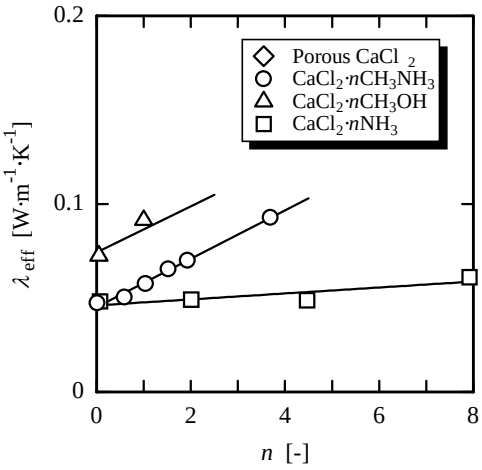

Fig.12 Variations of effective thermal conductivity with the moles n of gas substance reacted with $CaCl_2$.

The decrease in pellet void fraction ε_p with n, which has already been shown in Fig. 6, may lead to the increase in λ_{eff} with n. However the large decrease in λ_{eff} of the pellets at n=0 after thorough decomposition cannot be explained only by the decrease in ε_p since ε_p becomes smaller with increasing n. This suggests that the pellet thermal conductivity λ_p itself is probably decreased with n.

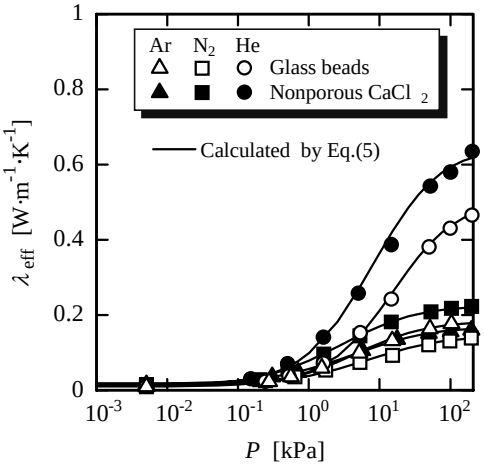

Fig.13 Variations of effective thermal conductivity with pressure (Glass beads D_p=60μm and nonporous $CaCl_2$ D_p=178μm)

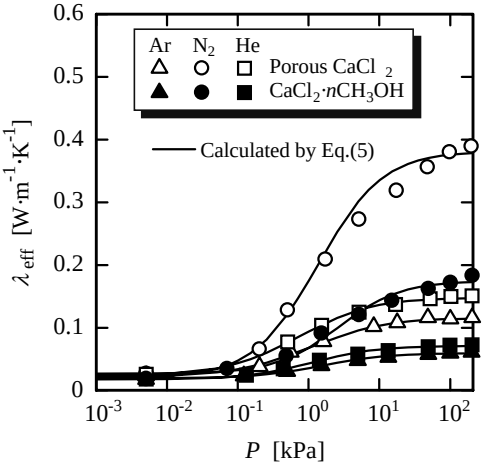

Fig.14 Variations of effective thermal conductivity with pressure (Porous CaCl2 Dp=675μm, and $CaCl_2 \cdot n CH_3OH$(n=0) Dp=305μm)

Variations of λ_{eff} with pressure P are shown in Fig.13 for nonporous pellets and in Fig.14 for porous pellets. At the pressure around 101.3 kPa, λ_{eff} varies largely depending on the substance in the gas phase. This means that the gas phase gives an appreciable contribution to heat transfer. λ_{eff} decreases with decreasing P, and it approaches the same value independent of the gas substance below 10 Pa.

4.3 Model for Effective Thermal Conductivity

Fujioka [14] proposed a model to estimate λ_{eff} by assuming that the bed is composed of an elementary cell shown in Fig.15. The cell consists of two adjoining spheres whose contact area is specified by angle ψ. Heat flow is assumed to take place in the vertical direction, and heat transfers by radiation and convection are neglected. Under these assumptions, heat flow through the cell is expressed by the following conductive heat transfer; (1) heat transfer through the gas phase in the void space, (2) heat transfer through the solid and gas phases near the contact surface in series and (3) heat transfer through the contact surface of the solid. Denote the part associated with mechanism (1) by I and that with mechanisms (2) and (3) by II, and the fractional area for heat transfer I and II by E and 1-E, respectively. Assuming that the region for part II is a cylinder with the diameter of D_p and the height of $D_p\cos\psi$ and neglecting the volume of contacting part, the volume of the solid sphere $(\pi/6)D_p^3$ is taken equal to $(1-\varepsilon_b)(\pi/4)D_p^3\cos\psi$ when E=0. Hence, the fractional area of part I is given by,

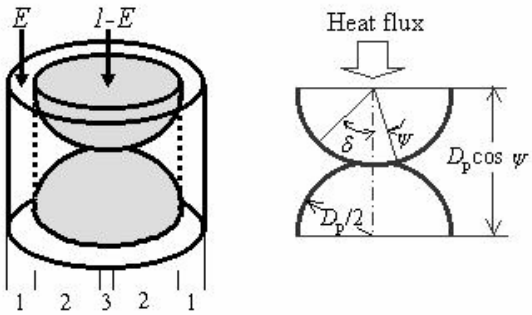

Fig.15 Heat transfer model for a packed bed

$$E = 1-(3/2)(1-\varepsilon_b)\cos\psi \qquad \text{for} \quad \varepsilon_b > 1-2/(3\cos\psi) \tag{4}$$

where E is set equal to zero when $\varepsilon_b \le 1-2/(3\cos\psi)$.

By introducing Kennard equation [17] for the pressure dependence of gas conductivity and deriving the expression for the heat flux in each part based on the models by Kunii and Smith [18] and Okazaki et al. [19], the effective thermal conductivity of bed is expressed by the following equation;

$$\lambda_{\mathrm{eff}} = E\frac{\lambda_{\mathrm{g}}^{\mathrm{o}}}{1+2\beta_{\mathrm{T}}\,L/\left(D_{\mathrm{p}}\cos\psi\right)} + \left(1-E\right)\left\{n_{\mathrm{c}}\,\lambda_{\mathrm{p}}\sin^2\psi + 2n_{\mathrm{c}}\,\lambda_{\mathrm{g}}^{\mathrm{o}}\cos\psi\left[\frac{\kappa}{\kappa-1}\left(\cos\delta_0-\cos\psi\right)\right.\right. + \left.\left.\left(\frac{\kappa}{\kappa-1}\right)^2\left(\cos\psi+2\beta_{\mathrm{T}}\,L/D_{\mathrm{p}}\right)\ln\frac{\kappa\left(\cos\psi+2\beta_{\mathrm{T}}\,L/D_{\mathrm{p}}\right)-\left(\kappa-1\right)\cos\delta_0}{\kappa\left(\cos\psi+2\beta_{\mathrm{T}}\,L/D_{\mathrm{p}}\right)-\left(\kappa-1\right)\cos\psi}\right]\right\} \quad (5)$$

where L denotes the mean free path of gas molecules, $\lambda_{\mathrm{g}}^{\mathrm{o}}$ is the normal gas thermal conductivity independent of pressure and β_{T} is so called 'temperature jump distance' in Kennard equation. n_{c} represents the effective number of contact points on a hemisphere for conductive heat transfer, $\kappa=\lambda_{\mathrm{p}}/\lambda_{\mathrm{g}}^{\mathrm{o}}$ and δ_0 denotes the angle indicating the boundary of each contact area. δ_0 is related to n_{c} by $1-\cos\delta_0=(1/n_{\mathrm{c}})^{1/2}$.

Estimation of effective thermal conductivity of nonporous pellet bed. Angle ψ can be obtained from the extrapolation of the measured λ_{eff} to P=0. In the case of nonporous pellets whose λ_{p} is equal to the solid thermal conductivity λ_{s}, the parameters of n_{c} and β_{T} are left unknown in Eq.(5). They were determined so as to minimize the sum of the squares of the deviations of the calculated λ_{eff} from the measured λ_{eff}. The calculations by Eq.(5) with n_{c} and β_{T} thus determined are shown by solid lines in Fig.13. The relations between n_{c} and ε_{b} almost coincide with the literature data for spherical pellets by Ridgway and Tarbuck [20] and that for nonspherical pellets by Okazaki et al. [19]. As shown in Fig.13 the calculated values are in good agreement with the measured λ_{eff} over the wide pressure range examined.

Estimation of pellet thermal conductivity of porous pellet. By using n_{c} thus obtained, the values of λ_{p} and β_{T} in Eq.(5) has been determined for porous pellets in the same procedure as described above. The calculations by Eq.(5) are shown in Fig. 14 by solid lines, and the pellet thermal conductivity λ_{p} determined in the procedure is plotted against n in Fig. 16. It should be noted that λ_{p} of the reactive pellets subjected to thorough desorption was considerably decreased from that of the unreacted $CaCl_2$ by repeating adsorption and desorption reactions.

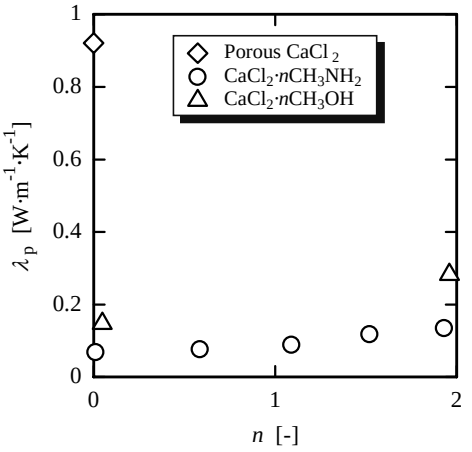

Fig.16 Relation between estimated pellet thermal conductivity and the moles n of reactive gas substance absorbed in one mole of $CaCl_2$.

44. Model for pellet thermal conductivity

The values of λ_{p}, which were derived from λ_{eff} measured in the gas phase of Ar, He or N_2, were almost independent of the gas phase substance. This means that heat mainly flows through the solid phase in a pellet. Further, the SEM photographs revealed that the shape and agglomerated state of grains in a pellet of reactive salt were considerably different from that of the unreacted $CaCl_2$, as shown in Fig.5.

In order to take account of such structural variations into the expression of λ_{p}, the unit cell model proposed by Luikov et al. [21] has been adopted in this study. The skeleton of the cell indicates the solid part, which is the shadowed portion shown in Fig.17. A pellet is composed of small nonporous grains and the cell represents a quarter of a grain. The contact resistance R_{c} to heat transfer is added to the upper and the lower surfaces of the cell in order to take account of the difference in contacting conditions of grains or the structural variations of the pellet shown in Fig.5. The model gives the following expression to λ_{p},

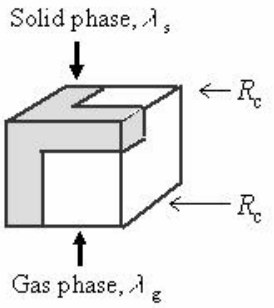

Fig.17 Unit cell for a pellet

$$\lambda_p = \frac{x^2}{R_c + 1/\lambda_s} + (1-x)^2 \lambda_g + x(1-x)\left[\frac{\lambda_s \lambda_g}{(1-x)\lambda_s + x\lambda_g + R_c \lambda_s \lambda_g}\right] \quad (6)$$

where λ_g denotes the gas thermal conductivity, λ_s the solid thermal conductivity and x the dimensionless thickness of solid skeleton related to ε_p.

Thermal conductivity of reactive pellet. The pellet thermal conductivity λ_p has been estimated from Eq.(6) for reactive and unreacted $CaCl_2$ pellets. In the estimation, λ_s of reactive solid was taken equal to 2.36 W/mK of the unreacted $CaCl_2$ in spite that the reactive salt is a complex of $CaCl_2$ and the absorbed reactive gas. The ground for this assumption is that the thermal conductivity of gas substance in a reactive solid will be close to that of the substance in solid state, as described in the sections of molar volume and the heat capacity of a reactive salt. there are few data to validate this assumption except for H_2O; λ_s of ice is 2.2 W/mK and λ_g^o of H_2O vapor is 0.0158 W/mK at 273 K, which is close to 0.0156 W/mK λ_g^o for of CH_3NH_2 and 0.0142 W/mK for λ_g^o of CH_3OH.

The relation between estimated λ_p and ε_p is shown in Fig.18 by solid lines together with λ_p determined from the measured λ_{eff}. Good agreement has been obtained by taking R_c=0 mK/W for the unreacted $CaCl_2$ and R_c=2 mK/W for the reactive pellets. The values of R_c have been selected so as to take account of the difference in grain structures observed in SEM photographs. In the unreacted $CaCl_2$ pellets, contact resistance seems to be negligible since the grains are partly fused in the pellet. On the other hand, such fusion or consolidation was not observed in the reactive pellets. The contact resistance between reactive grains probably has led to a significant decrease in λ_p. This is the reason why λ_p of reactive solid with n=0 after thorough decomposition becomes much smaller than that of the unreacted $CaCl_2$.

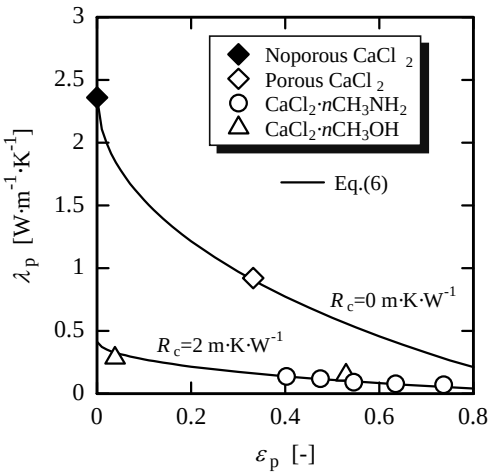

Fig.18 Relation between pellet thermal conductivity and pellet void fraction

4.5 Estimation of Effective Thermal Conductivity.

Since the parameters in Eq. (5) have been determined as described above, it is now possible to estimate λ_{eff} of a bed packed with $CaCl_2$ salt under various conditions. Figure 19 shows a comparison of λ_{eff} estimated by Eq. (5) with measured λ_{eff} for a bed of $CaCl_2 \cdot nCH_3NH_2$. In this comparison, the condition for the gas phase was not the same. The gas phase was nitrogen at 101.3 kPa for $n \le 2$, but it was methylamine for n>2. The pressure was adjusted so that the reactive salt was kept in an equilibrium state, that is, from 12 kPa to 20 kPa for n=4 and about 35 kPa for n=6. n of the sample salt at the equilibrium pressure for n=6 was less than 6, since it was difficult to prepare a salt fully reacted with methylamine. As shown in Fig.19, agreement of Eq. (5) with the measurements is satisfactory.

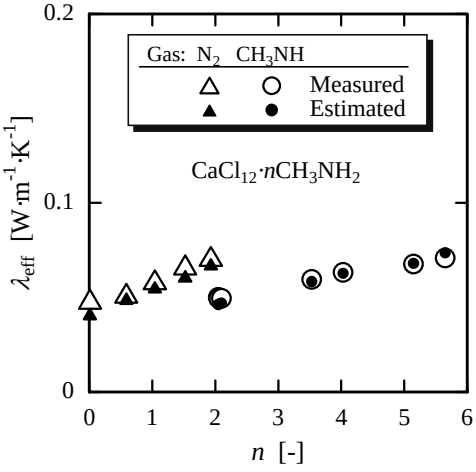

Fig.19 Comparison of measured and estimated thermal conductivities of $CaCl_2 \cdot nCH_3NH_2$

5. SUMMARY

The molar volume and heat capacity of $CaCl_2 \cdot nNH_3$, $CaCl_2 \cdot nCH_3NH_2$ or $CaCl_2 \cdot nCH_3OH$ increase proportionally with n. The variations in these properties are inherent in each substance

absorbed in the salt irrespective of the kind of salt and expressed by the additivity of the properties of the unreacted salt to those of the absorbed substance in a condensed phase.

SEM observation revealed that a pellet of $CaCl_2 \cdot nCH_3OH$ was an agglomerate of small grains and the shape of a grain transformed from round to angularly slender as the adsorption/desorption reaction was repeated. Bed void fraction and pellet void fraction have been introduced in order to characterize heat transfer in a porous pellet bed. In a freely expanding bed with constant bed void fraction, the pellet void fraction was decreased with the progress of adsorption reaction.

Effective thermal conductivity of a bed of $CaCl_2$ salt was reduced to less than a half that of the initial anhydrous $CaCl_2$ bed by reaction, which was presumed to be caused by a decrease in the thermal conductivity of the salt itself. A model to estimate effective thermal conductivity of a bed packed with porous pellets and pellet thermal conductivity has been developed by extending the previous models proposed by Kunii and Smith, Okazaki et. al., and Luikov et al.. The equations derived from the model represent appropriately the effects of gas pressure, gas thermal conductivity and void fraction on the effective thermal conductivity. In addition, the model expresses well the significant decrease in the pellet thermal conductivity due to reaction by taking account of the changes in structure of agglomerated grains in a pellet in terms of contact resistance to heat transfer through it.

It is usual that temperature and pressure has to be changed in a reactor when the reaction is reversed between the adsorption and desorption reactions. The model developed in this study will enable one to estimate heat transfer properties of a reactor bed that is operated under a condition accompanied with large variations of temperature and pressure to drive a chemical heat pump.

Acknowledgement
The authors are grateful for the financial support from Ministry of Education, Science, Sports and Culture of Japan for Grant-in-Aid for Priority Areas (No.06246216)

Nomenclature

Cp : molar heat capacity [$J \cdot mol^{-1} \cdot K^{-1}$]
D_p : particle diameter [m]
E : portion of heat transfer through gas phase in a packed bed by Eq. (4) [-]
L : mean free path [m]
n : moles of gas substance reacted with one of salt [mole]
n_c : contact number [-]
R_c : contact resistance to heat transfer in a cell of pellet
V : volume [m^3]
V_b : bed volume [m^3]
V_m : molar volume [$m^3 \cdot mol^{-1}$]
V_p : pellet volume [m^3]
x : portion of solid stem in a cell of pellet [-]
β : increase in molar volume of salt per one mole of gas reacted with it [$m^3 \cdot mol^{-1}$]
β_Γ : temperature jump distance [-]
ε : overall void fraction [-]
ε_b : bed void fraction [-]
ε_p : pellet void fraction [-]
γ : increase in heat capacity of salt per one mole of gas reacted with it [$J \cdot mol^{-1} \cdot K^{-1}$]
λ : thermal conductivity [$W \cdot m^{-1} \cdot K^{-1}$]
λ_{eff} : effective thermal conductivity [$W \cdot m^{-1} \cdot K^{-1}$]
λ_g^o : thermal conductivity of gas [$W \cdot m^{-1} \cdot K^{-1}$]
λ_p : thermal conductivity of pellet [$W \cdot m^{-1} \cdot K^{-1}$]
λ_s : thermal conductivity of solid phase [$W \cdot m^{-1} \cdot K^{-1}$]
Ψ : contact angle of two adjacent grains [radian]

Subscript
b : bed
g : gas
s : solid

References

1. Gillespie, L., Gerry, H.T., Densities and Partial Molar Volumes of Ammonia for the Ammines of Calcium and Barium Chlorides, *Journal of American Chemical Society*, 1931, Vol. 53, pp. 3962-3968.
2. Mauran, S., Prades, P., F. L'Haridon, Heat and Mass Transfer in Consolidated Reaction Beds for Thermochemical Systems, *Heat Recovery Systems & CHP*, 1993, Vol.13, pp.315-319.
3. Oms, J.L., Identification des Paramètes Thermiques d'un Milleu Poreuz Réactif Déformable Application aux Pompes à Chaleur Chimiques Solide-gaz, *Rev. Gén. herm. Fr.*, 1991, pp.354-355.
4. Goetz, V., Marty, A., A model for Reversible Solid-gas Reactions Submitted to Temperature and Pressure Constraints: Simulation of the Rate of Reaction in Solid-gas Reactor Used as Chemical Heat Pump, *Chemical Engineering Science*, 1992, Vol. 47, pp. 4445-4454.
5. Lourdudoss, S., Schuler, T., Raldow, W., Determination of the Heat Capacity of Calcium Chloride Octa- and Tetraamines, *Inorganica Chimica Acta*, 1981, Vol.54, pp. 31-33.
6. Marty, A., Etude par Microcalorimetric de la Reactive de Deux Ammoniacates de chlorure de Manganese, *Jounal of Thermal Analysis*, 1991, vol. 37, pp. 479-498.
7. Mazet, N, Amouroux, M., Analysis of Heat Trasnfer in a Non-isothermal Solid-gas Reacting Medium, *Chemical Engineering Science*, 1991, Vol. 99, pp.175-200.
8. Guilleminot, J.J., Heat Transfer Intensification in Fixed Bed Adsorbers, *Heat Recovery Systems & CHP*, 1993, Vol. 13, pp. 297-300.
9. Groll, M., Reaction Beds for Dry Sorption Machines, *Heat Recovery Systems & CHP*, 1993, Vol. 13, pp. 341-346
10. Kanzawa, A., Arai, Y., Thermal Energy Storage by the Chemical Reaction – Augmentation of Heat Transfer and Thermal Decompositon in the CaO/Cc(OH)2 Powder-, Solar Energy, 1981, Vol.27, pp. 289-294.
11. Ogura, H., Miyazaki, M., Matsuda, H., Hasatani, M., Yanadori, M., Hiramatsu, M., Experimental Study on Heat Transfer Enhancement of the Solid Reactant Particle Bed in A Chemical Heat Pump Using Ca(OH)2/Cao Reaction (in Japanese), Kagaku Kogaku Ronbunshu, 1991, Vol.17, 916-923.
12. Fujioka K., Kato, S., Fujiki, S., Hirata, Y., Variations of Molar Volume and Heat Capacity of Reactive Solids of $CaCl_2$ used for Chemical Heat Pumps, *Journal of Chemical Engineering of Japan*, 1996, pp. 858-864.
13. Landolt-Börnstein, Zahrenwerte und Funktion aus Phsik, Chemie, Astronomi, Geophysik und Technik, 1971, 6, Aufl., Bd. II/I, Springer-Verlag
14. Fujioka, K., Thermophysical Properties and Heat Transfer Mechanism of $CaCl_2$ Reactor Bed for Chemical Heat Pump, 1999, Doctor Thesis (Osaka University)
15. The Chemical Society of Japan, Kagaku-Binran Kisohen II (in Japanese), 3rd. ed., Maruzen, Japan, 1984, pp. 240-246 and p.251.
16. Fujioka, K., Kato, S. and Hirata, Y., Measurements of Effective Thermal Conductivity of CaCl2 Reactor Beds Used for Driving Chemical Heat Pumps, *Journal of Chemical Engineering of Japan*, 1998, Vol. 31, pp. 266-272
17. Kennard, E.H., Kinetic Theory of Gases, McGraw-Hill, New York and London, 1938
18. Kuii D., Smith, J.M., Heat Transfer Characteristics of Porous Rocks, *AIChE Journal*, 1960, Vol.6, pp. 71-78
19. Okazaki, M., Ito, I., Toei, R., Effective Thermal Conductivities of Wet Granular Materials, *AIChE, Symposium Series*, 1977, Vol. 163, pp.164-176
20. Ridgway,K., Tarbuck, K.J., The Random Packing of Spheres, British Chemical Engineering, 1967, Vol. 12, p.384.
21. Luikov, A.V., Shashkov, A.V., Vasiliev, L.L., Fraiman, Yu.E., Thermal Conductivity of Porous Systems, *Inter. J. Heat Mass Transfer*, 1968, Vol.11, pp.117-140